

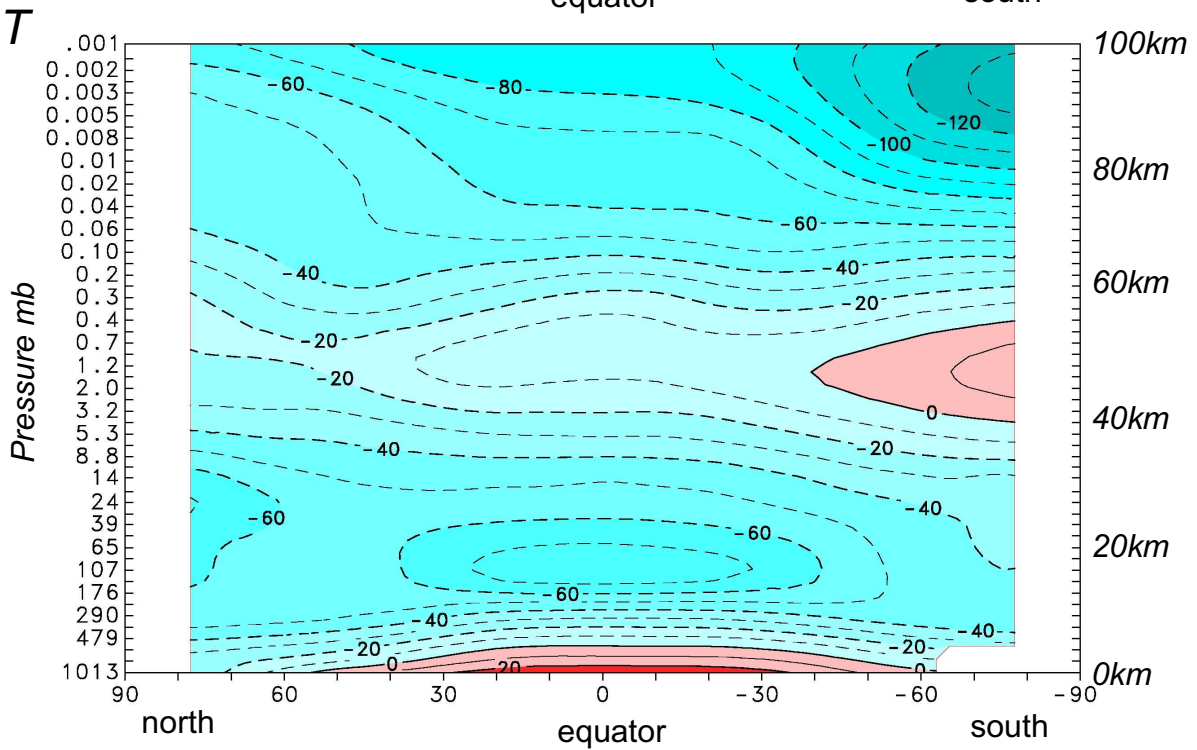
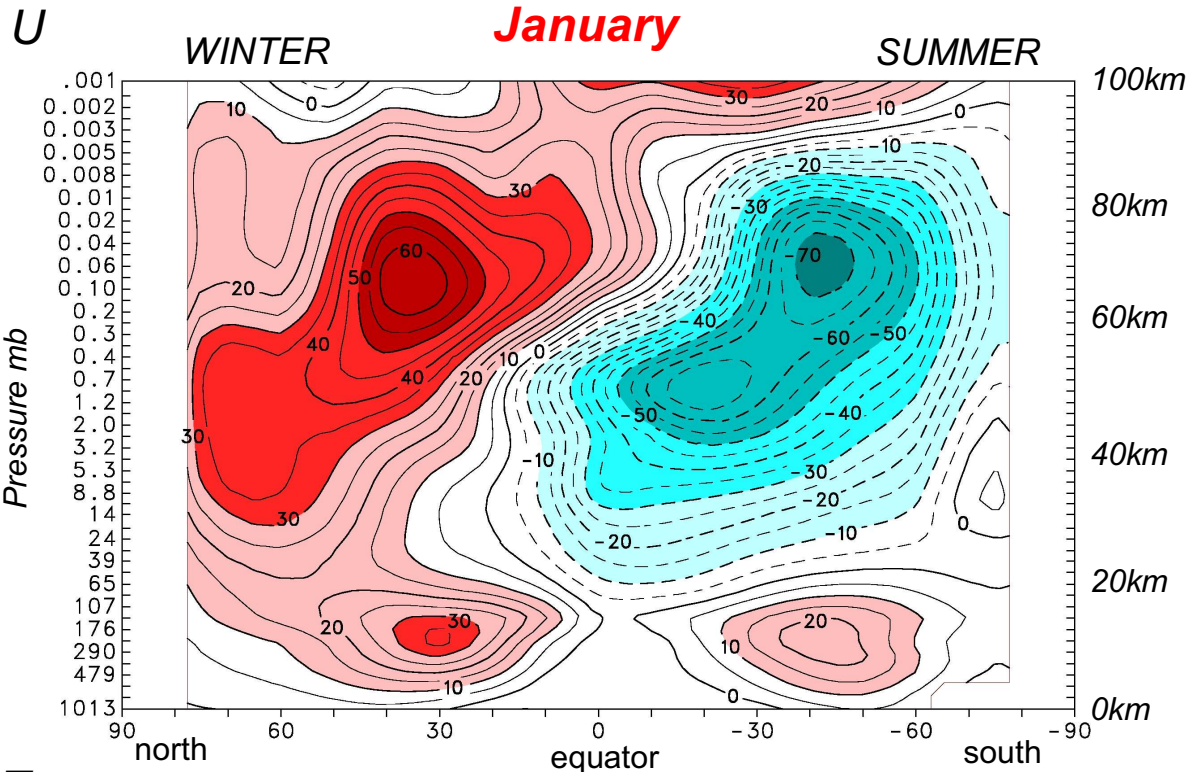
Atmospheric Tracer Transport

John Scinocca

*CCCma, MSC
Victoria*

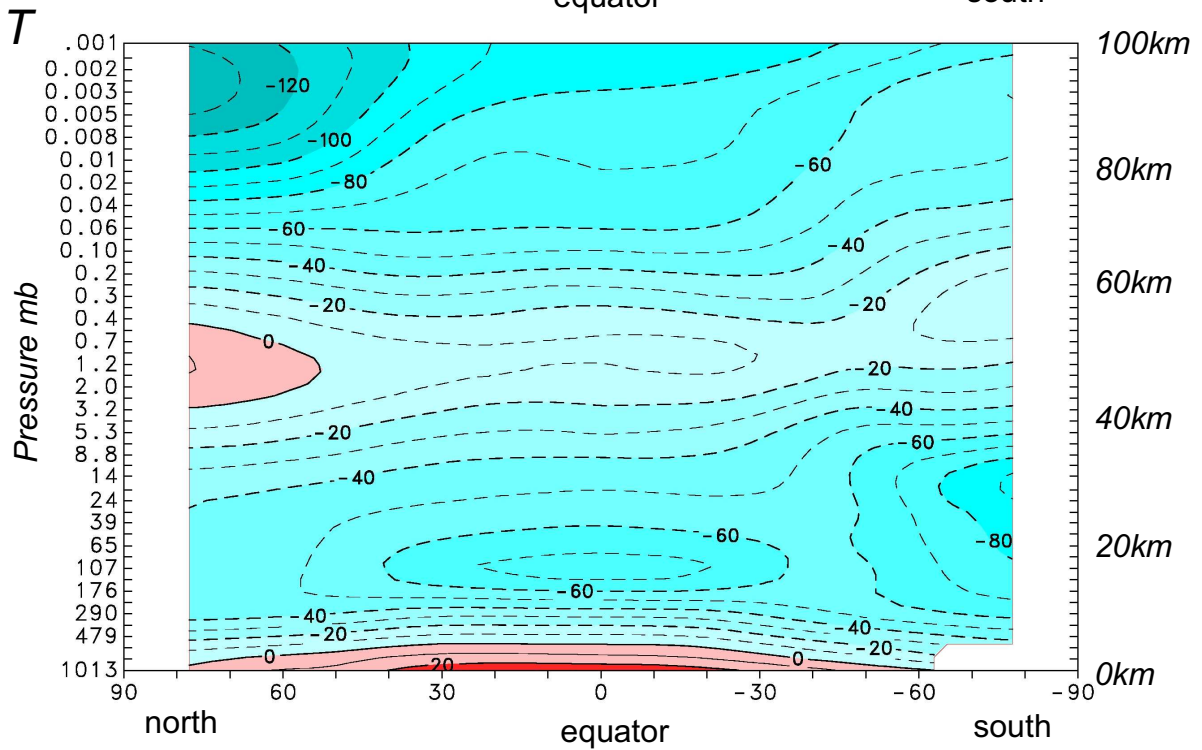
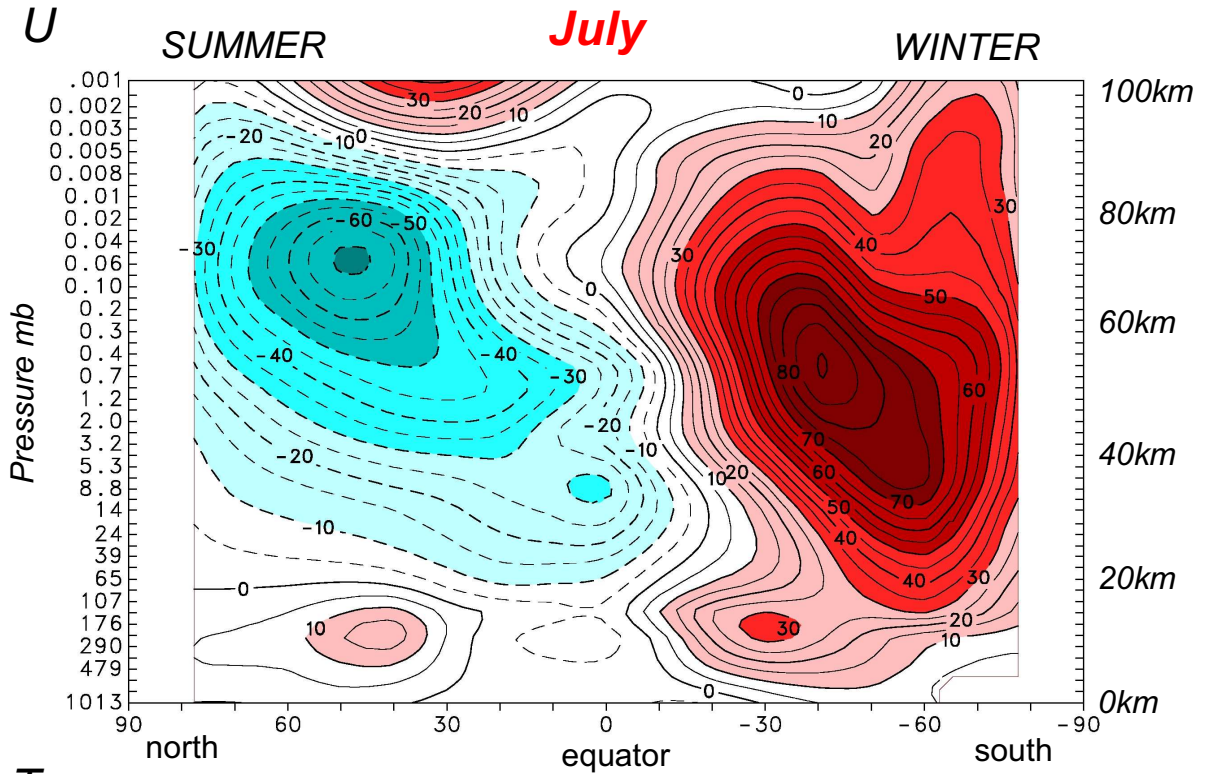
- *U and T structure of the Atmosphere*
- *Mass Mixing Ratio vs Mass of Tracer*
- *Paradigms of Mixing: Chaotic vs 3D Turbulent Mixing*
- *Advection Diffusion Equation*
- *Isentropic coordinates*
- *Quasi 2D Transport*
- *Local Mixing and Barriers to Transport*
- *Contour Advection*
- *Global Picture of Large-Scale Transport*
- *Effective Diffusivity*

U and T of Troposphere and Stratosphere



Cira Data

U and T of Troposphere and Stratosphere



Cira Data

Tracer Advection

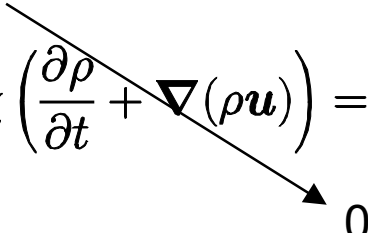
total mass conservation:

$$\frac{\partial \rho}{\partial t} + \nabla(\rho \mathbf{u}) = 0$$

tracer χ mass equation:

$$\frac{\partial \rho_\chi}{\partial t} + \nabla(\rho_\chi \mathbf{u}) = S$$

– define “mass mixing ratio” $\chi \equiv \rho_\chi / \rho$ $\rho_\chi = \chi \rho$

$$\rho \left(\frac{\partial \chi}{\partial t} + \mathbf{u} \cdot \nabla \chi \right) + \chi \left(\frac{\partial \rho}{\partial t} + \nabla(\rho \mathbf{u}) \right) = S$$


$$\frac{D\chi}{Dt} = \frac{\partial \chi}{\partial t} + \mathbf{u} \cdot \nabla \chi = S/\rho$$

Two Paradigms for Stirring and Mixing

Chaotic Advection

large-scale “slow” (balanced) motions

– *Stirring and mixing are mediated by large-scale eddies. The flow varies smoothly in space and time with a well-defined length scale.*

⇒ *eddy turnover time is the same at all scales*

Small-scale filamentary structure develops in tracers on a time scale that is long compared to the time scale for the advection.

⇒ *advection may spread tracers over a long distance prior to mixing*

3D Turbulence

boundary layer, convection, intermittent mixing events (internal-wave breaking)

forcing scale
(large)

inertial range

dissipation scale
(small)



– *In the inertial range, stirring and mixing at any scale are mediated by eddies at that scale.*

⇒ *eddy turnover time decreases as scale decreases*

time scale for turbulent mixing is the same order as the time scale for advection

⇒ *3D turbulence is very effective at mixing*

Real Atmosphere

In general, rotation and stratification inhibit 3D turbulence on the large scale in the atmosphere.

above the boundary layer there is no background field of 3D turbulence only the net effect of localized sporadic events (I.e., convection, shear instability, breaking gravity waves)

⇒ Chaotic mixing dominates the troposphere and stratosphere

But! molecular diffusion is enhanced by intermittent events of 3D turbulence (more important in the troposphere)

→ focus on chaotic transport from here on

Tracer Stirring and Mixing

tracer evolution: advection diffusion equation

$$\frac{\partial \chi}{\partial t} + \mathbf{u} \cdot \nabla \chi = \kappa \nabla^2 \chi$$

scale analysis: $\frac{\chi U}{L} \quad \frac{\kappa \chi}{L^2}$

Peclet number: $Pe = \frac{UL}{\kappa} \quad \frac{\text{advection}}{\text{diffusion}}$

large Pe \Rightarrow advection dominates diffusion

$$\kappa \sim \begin{cases} 10^{-3} \text{m}^2 \text{s}^{-1} & (\text{troposphere}) \\ 10^{-5} \text{m}^2 \text{s}^{-1} & (\text{stratosphere}) \end{cases}$$

$$L \sim 100 \text{m}$$

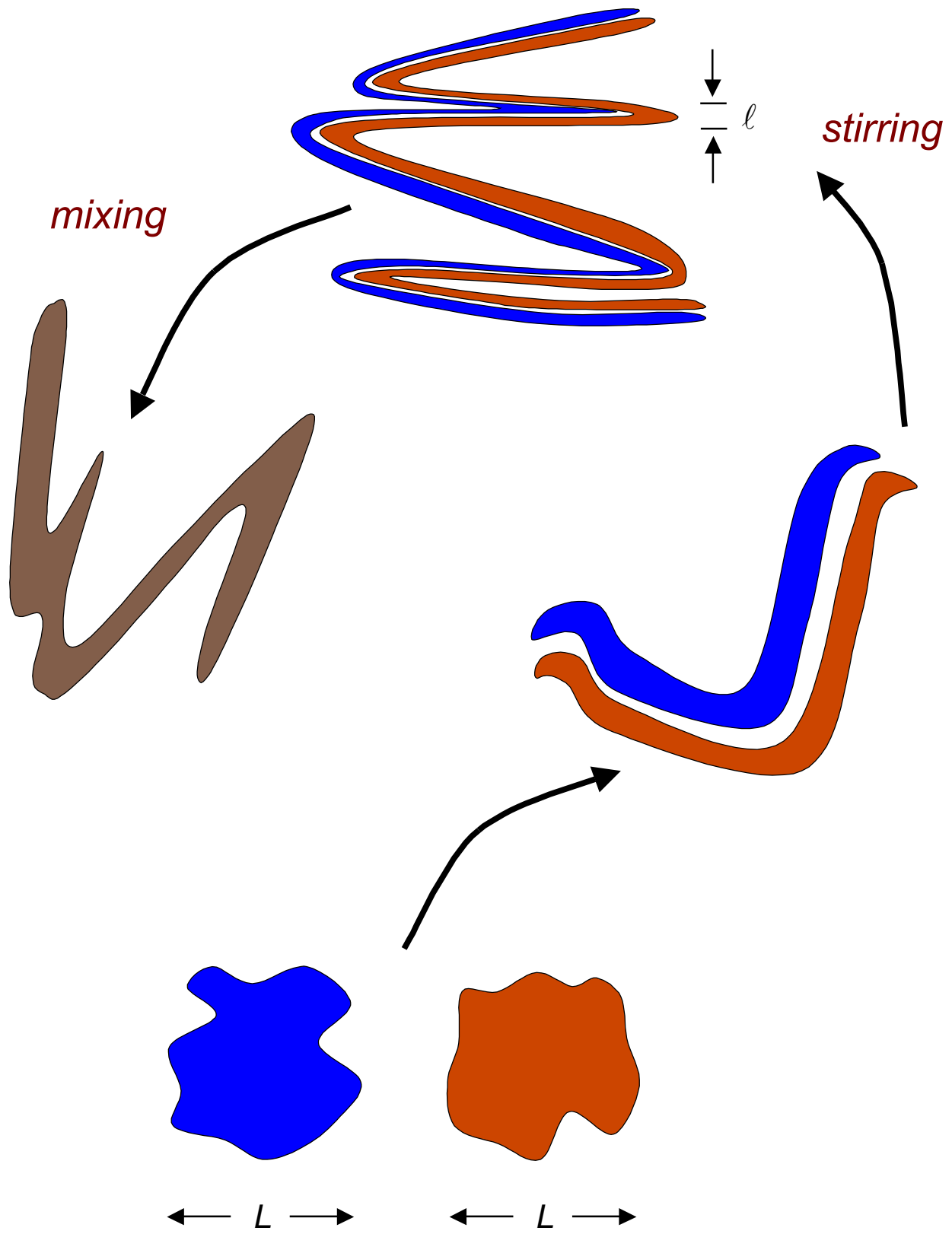
$$T \sim \frac{L^2}{\kappa} \sim 10^8 \text{s} \quad \Rightarrow \text{several years to homogenize tracers over a distance of } 100 \text{m}$$

stirring enhances diffusion by reducing length scale of χ

$$\frac{\kappa \chi}{L^2} \rightarrow \frac{\kappa \chi}{l^2} \Rightarrow \frac{\kappa}{l^2} \sim \frac{U}{L}$$

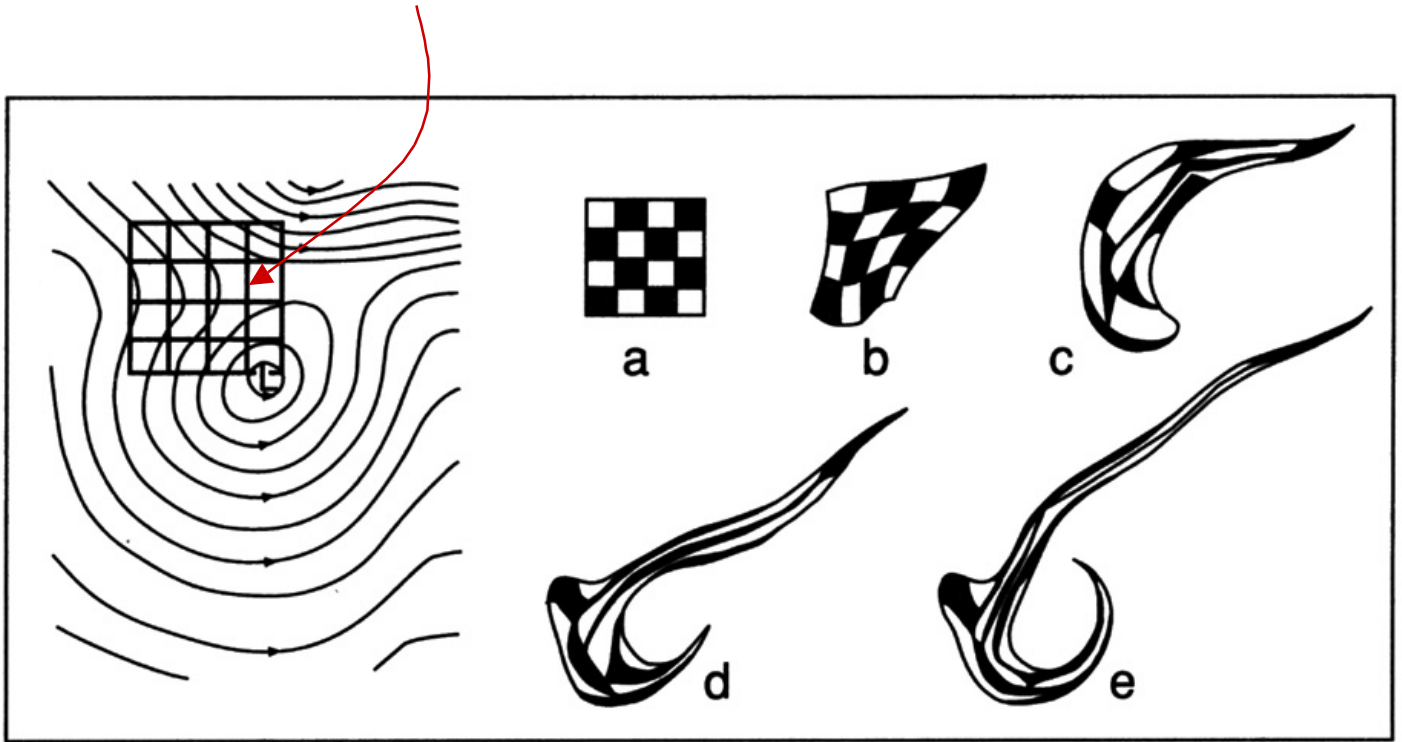
$$l \sim \left(\frac{\kappa L}{U} \right)^{1/2} = L Pe^{-1/2}$$

Chaotic Transport: Stirring and Mixing



Chaotic Stirring

stagnation point in large-scale flow



stagnation points are very effective at stirring tracers

Isentropic Coordinates

$$\frac{D\theta}{Dt} = Q$$

Q – diabatic processes (radiation, molecular dissipation)

θ is a monotonic function of height and so can be used as a vertical coordinate

⇒ focus attention on whether parcel motion is diabatic (reversible) or adiabatic (irreversible)

time scale of diabatic processes 10–20 days

⇒ on time scales of several days neglect diabatic effects and consider transport (stirring and mixing) along isentropic surfaces

$$\frac{D\theta}{Dt} = 0$$

⇒ 3D transport problem now reduced to a 2D transport problem

2D nature of balanced dynamics in isentropic coordinates (e.g., QG dynamics) implies close parallel with 2D vortex dynamics:

$$\frac{D\zeta}{Dt} = \frac{\partial\zeta}{\partial t} + J(\psi, \zeta) = 0$$
$$\psi = \nabla^{-2}\zeta$$

$$\zeta = \nabla^2\psi$$

$$(u, v) = \left(-\frac{\partial\psi}{\partial y}, \frac{\partial\psi}{\partial x} \right)$$

$$J(\psi, \zeta) = \left(\frac{\partial\psi}{\partial x} \frac{\partial\zeta}{\partial y} - \frac{\partial\zeta}{\partial x} \frac{\partial\psi}{\partial y} \right)$$

Quasi-2D Transport (Stratosphere)

PV reveals spatial structure of transport (stirring and mixing) along isentropic surfaces

Two basic regimes:

reversible deformations of PV: upward propagation of Rossby waves on polar night jet (winter stratosphere)

associate with strong PV gradients

irreversible deformations of PV: low-latitude Rossby-wave breaking “surf-zone” (winter stratosphere)

associate with weak PV gradients

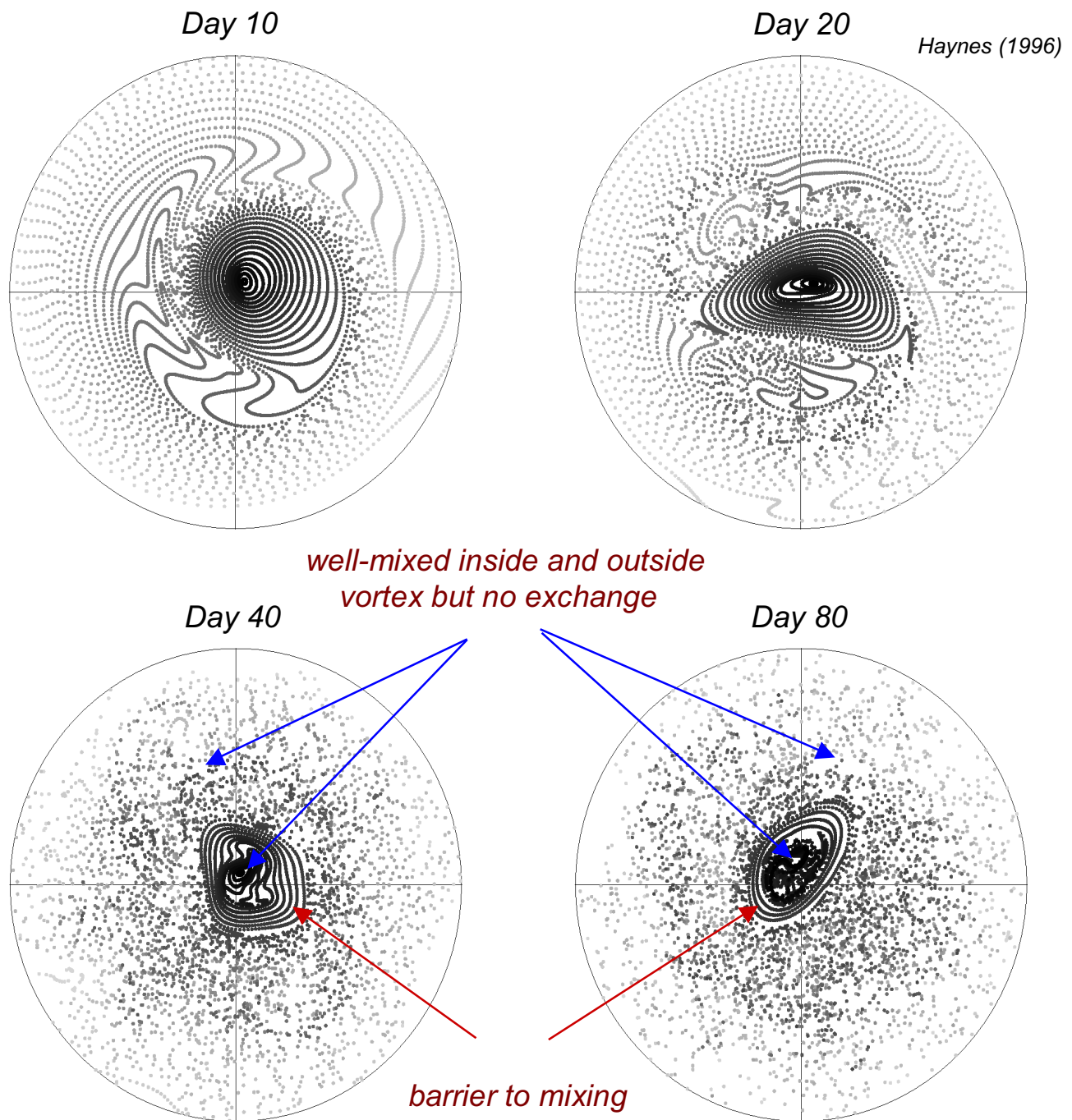


Figure 4: Tracer particles advected in a dynamically consistent numerical simulation of single-layer flow on a sphere. The flow is viewed from above the North pole. The particles are shaded according to their initial latitude, with darker shading corresponding to higher latitude. The flow consists of a strong cyclonic (anti-clockwise) vortex at high latitudes, disturbed by a large-scale forcing centred at mid latitudes. The amplitude of the forcing is smoothly increased from zero at the beginning of the simulation and is smoothly decreased and then increased again, with a period of 20 days, as the simulation progresses. Particles are shown at (a) 10 days, (b) 20 days, (c) 40 days, and (d) 80 days. It may be seen that there is a systematic adjustment of the particles to a statistically quasi-steady state where they are apparently well-mixed outside the vortex and inside the vortex, but there is no exchange across the vortex boundary.

Localized Stirring and Mixing

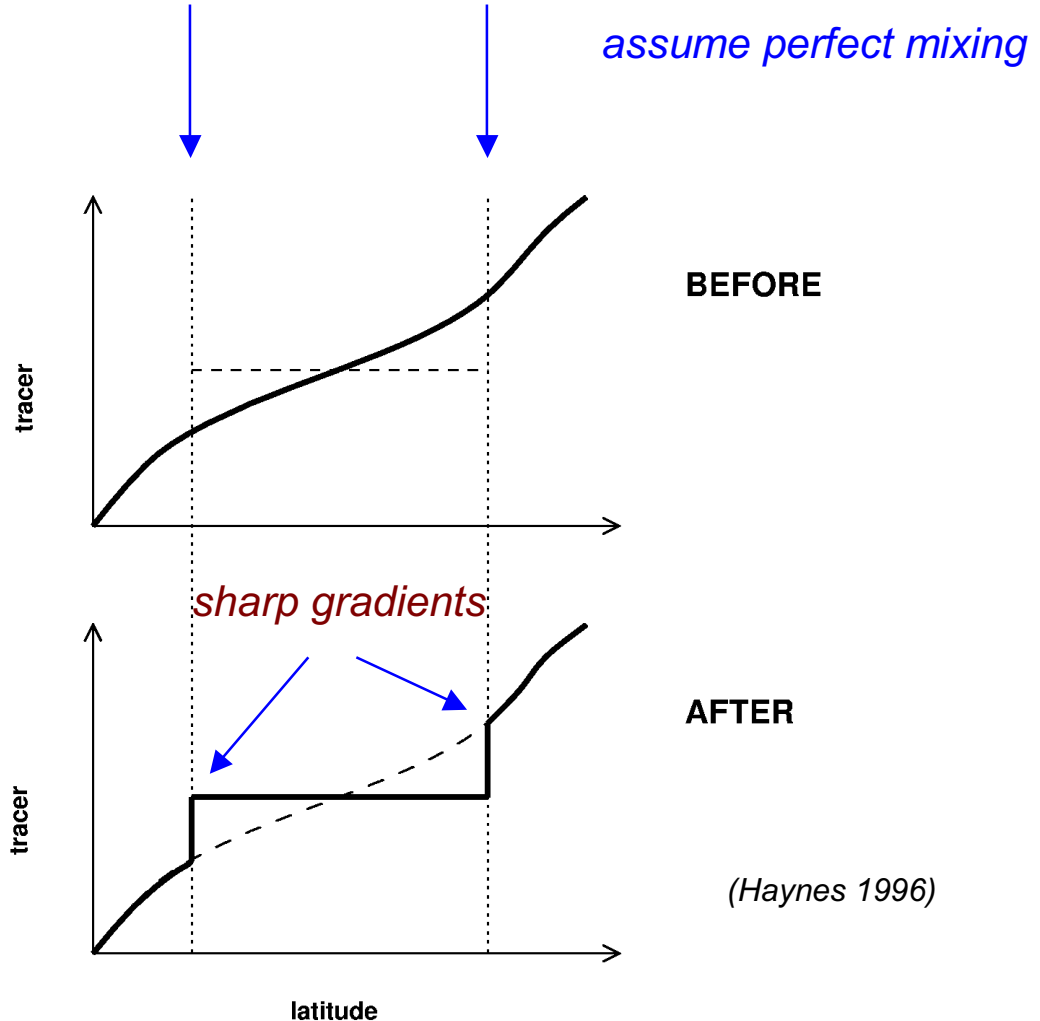


Figure 5: Effect of localized stirring on a tracer distribution. The variation with latitude of initial tracer distribution is shown by the solid curve. The tracer is assumed subsequently to be stirred (and perfectly mixed) over a limited range of latitudes, bounded by the finely dashed lines. The effect of the localised stirring and the resultant mixing is not only to make the tracer constant in this region, but also to produce sharp tracer gradients at the edges of the region.

sharp gradients of passive tracers \Rightarrow *sharp gradient of PV*

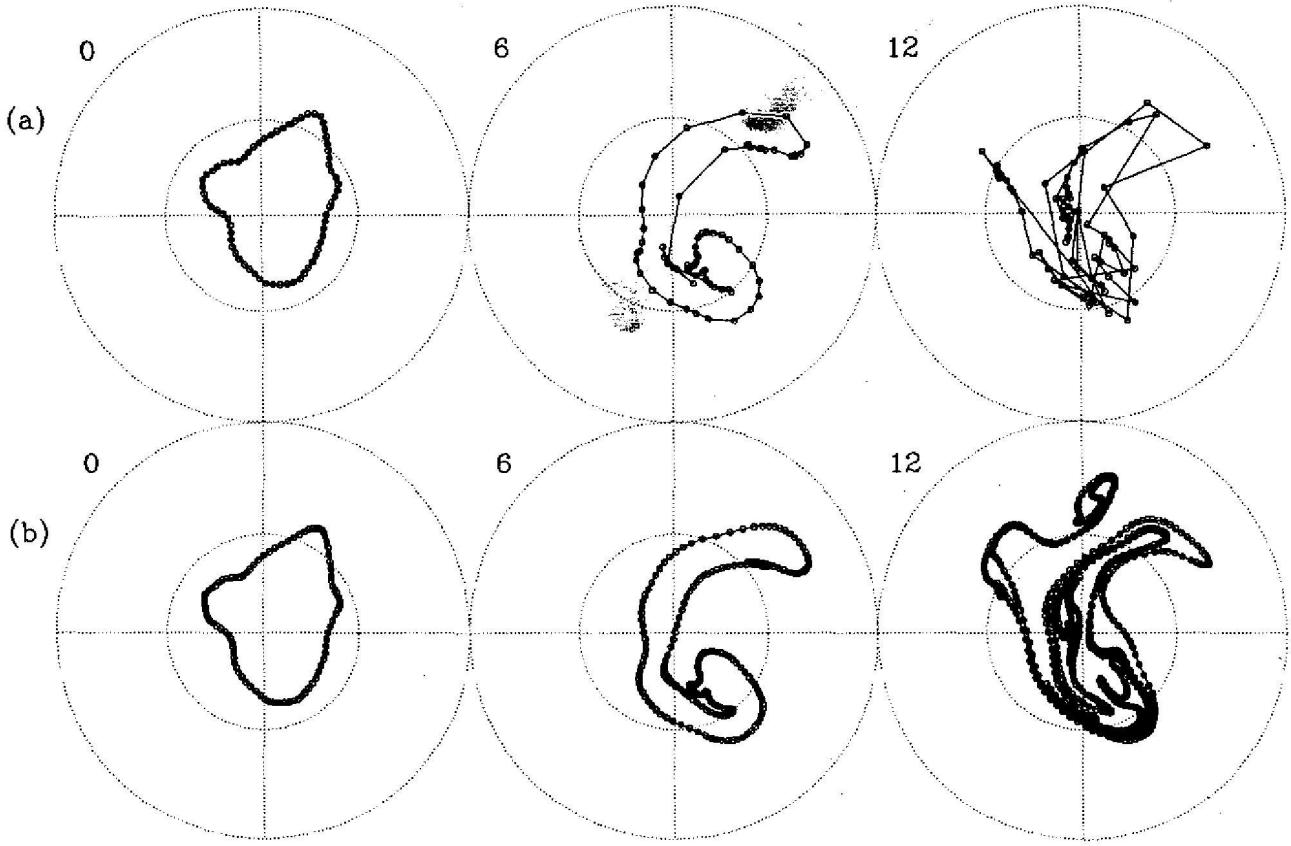
PV restoring force \propto to PV gradient ("PV elasticity")
difficult to irreversibly deform strong PV gradients

\Rightarrow *Strong PV gradients tend to be barriers to transport*

Contour Advection Algorithms (CAS)

(Waugh and Plumb 1994)

particle advection →



← *contour advection*

application of CAS to model output (SKYHI)

(Vaugh and Plumb 1994)

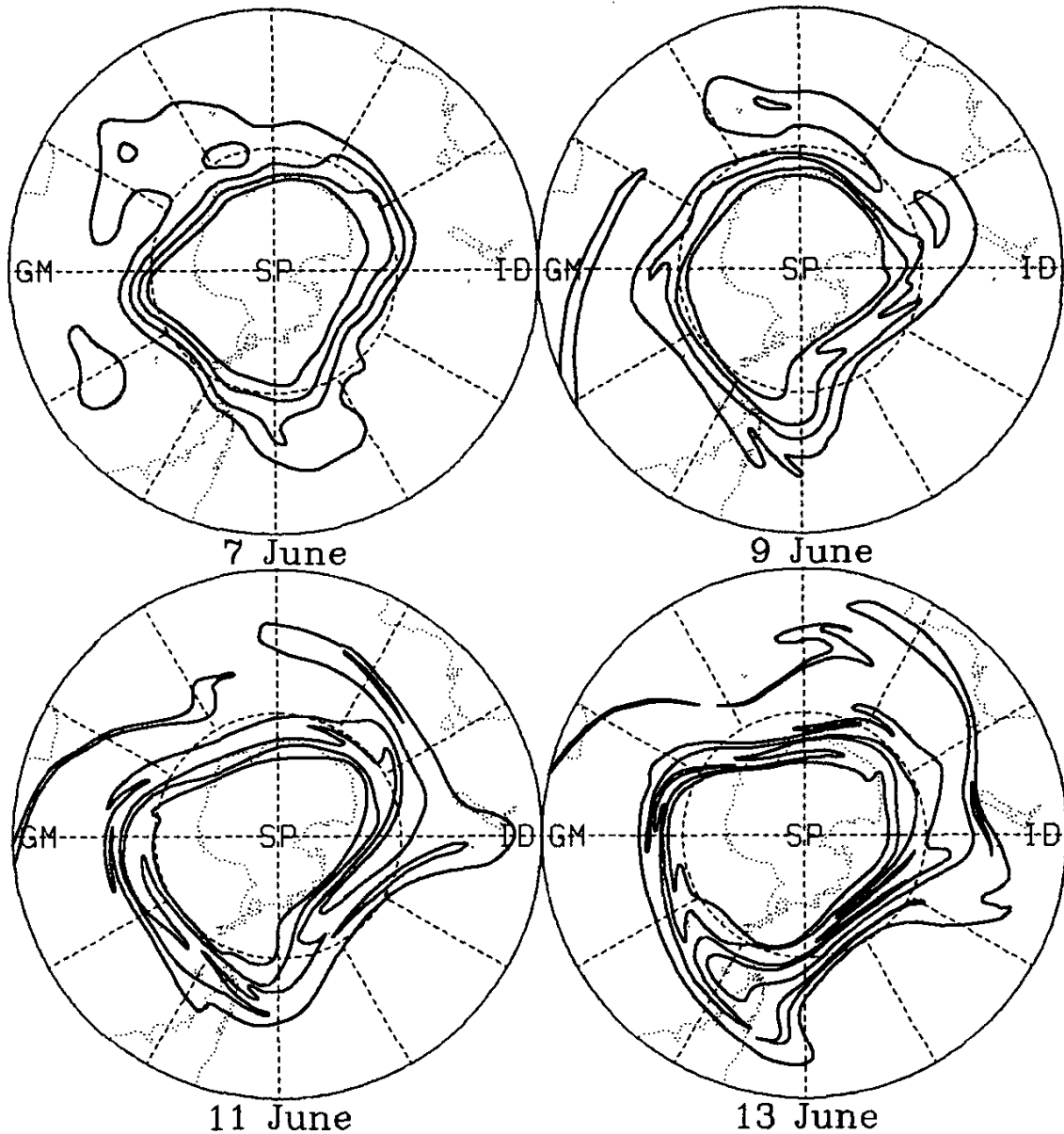
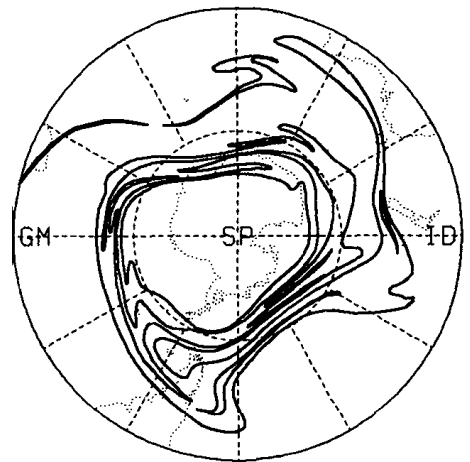


FIG. 6. Output from a 6-day CAS calculation using SKYHI data. At the start of the calculation the contours correspond to PV contours $Q = (-1.8, -2.0, -2.2, -2.4) \times 10^{-5} \text{ K m}^2 \text{ g}^{-1} \text{ s}^{-1}$ on the 450 K isentropic surface at 0300 UTC 7 June. The advecting velocity field has spatial resolution $\Delta\phi \times \Delta\lambda = 1^\circ \times 1.2^\circ$, and temporal resolution $\Delta T = 12 \text{ h}$. Plots are polar stereographic projections; latitudinal circles 30°S (solid) and 60°S (dashed) are marked.

illustration of chaotic nature of transport

(Waugh and Plumb 1994)

wind resolution: $\Delta\phi \times \Delta\lambda = 1^\circ \times 1.2^\circ$
 $\Delta t = 12\text{hr}$

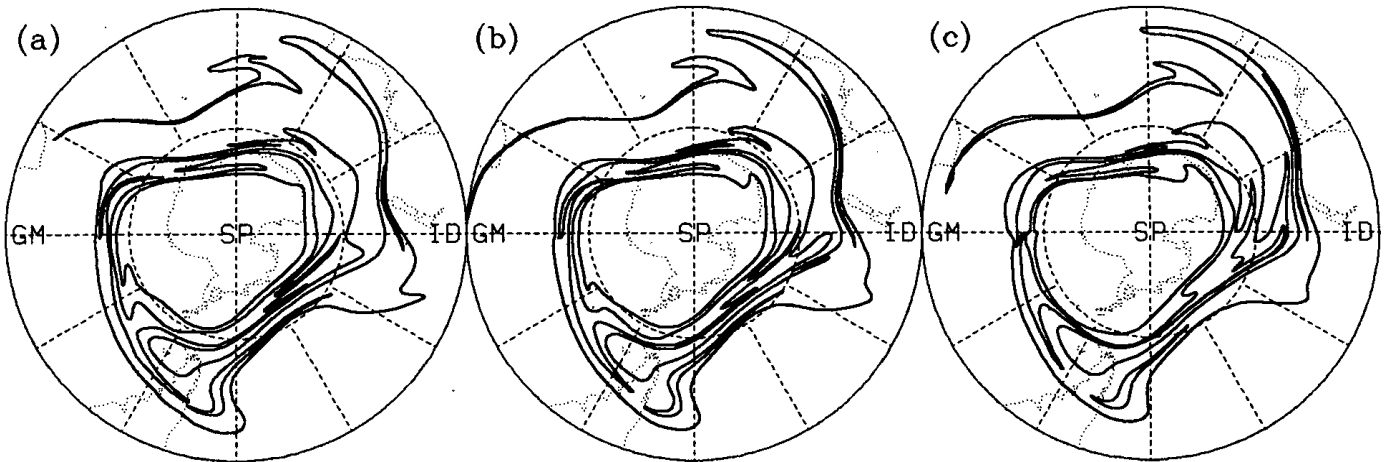


$\Delta t = 12\text{hr}$

$3^\circ \times 3.6^\circ$

$5^\circ \times 6^\circ$

$10^\circ \times 12^\circ$

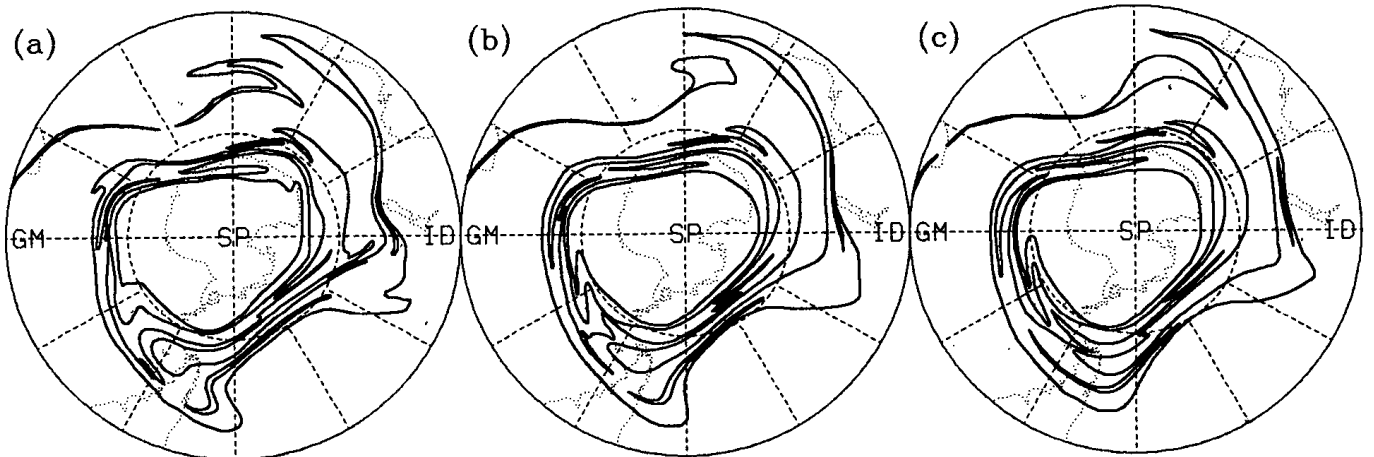


$\Delta\phi \times \Delta\lambda = 1^\circ \times 1.2^\circ$

$\Delta t = 6\text{hr}$

$\Delta t = 24\text{hr}$

$\Delta t = 48\text{hr}$

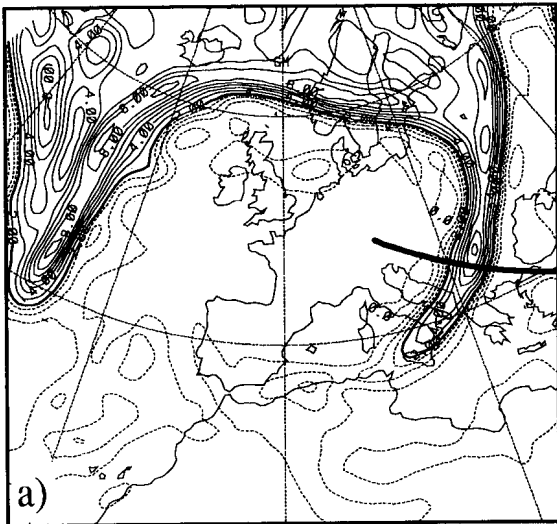


(Appenzeller et al. 1996)

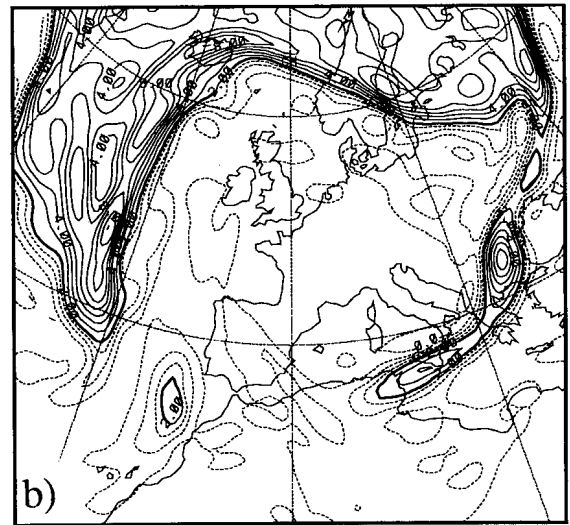
ECMWF analysis data T213/L31

diagnosed PV

PV 320K 13/ 5/92 0GMT



PV 320K 13/ 5/92 12GMT

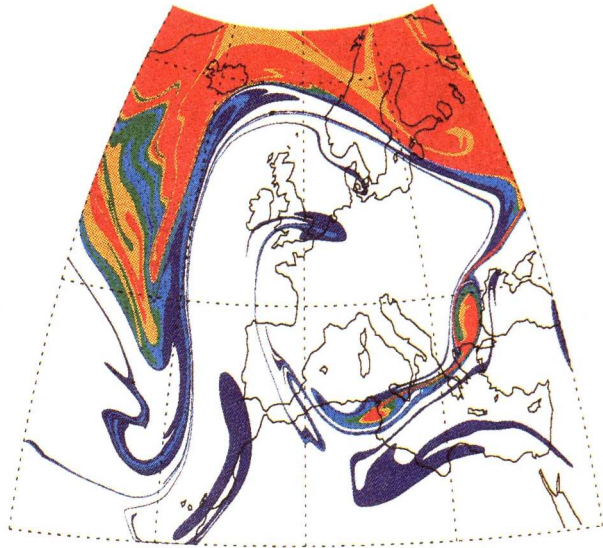


CAS algorithm PV using winds T106 initialized 4 days earlier

DAY 92051300



DAY 92051312



(Appenzeller et al. 1996)

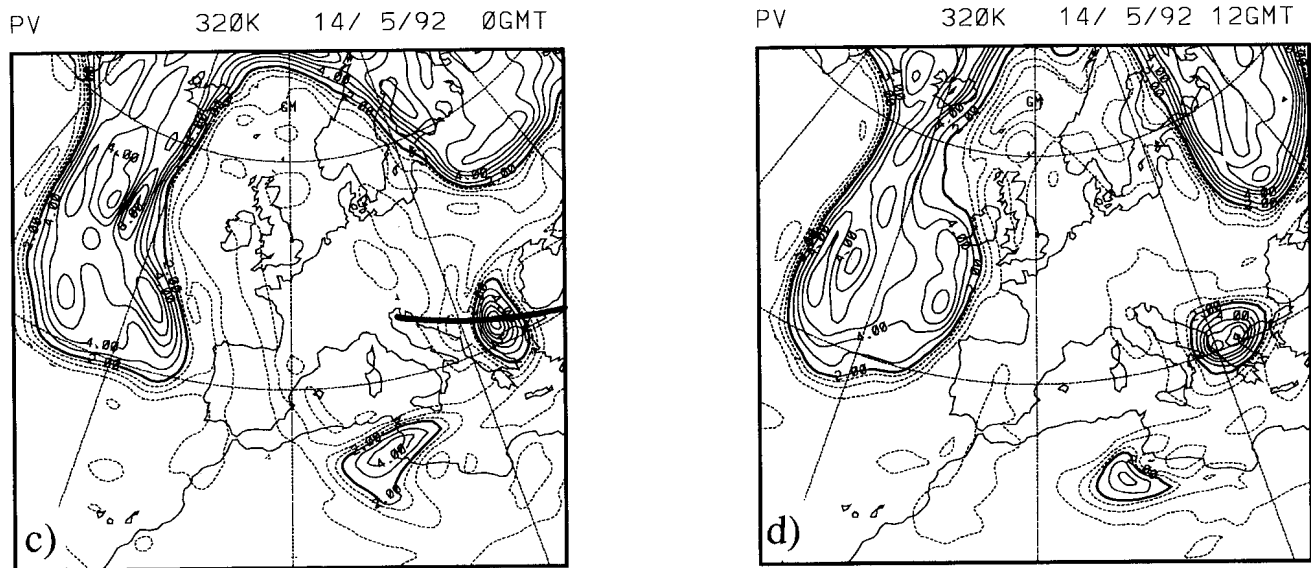


Figure 7. The PV field on a $\theta = 320$ K surface at 12-hour intervals from 0000 UT, May 13, 1992. (Contour convention as for Figure 2).

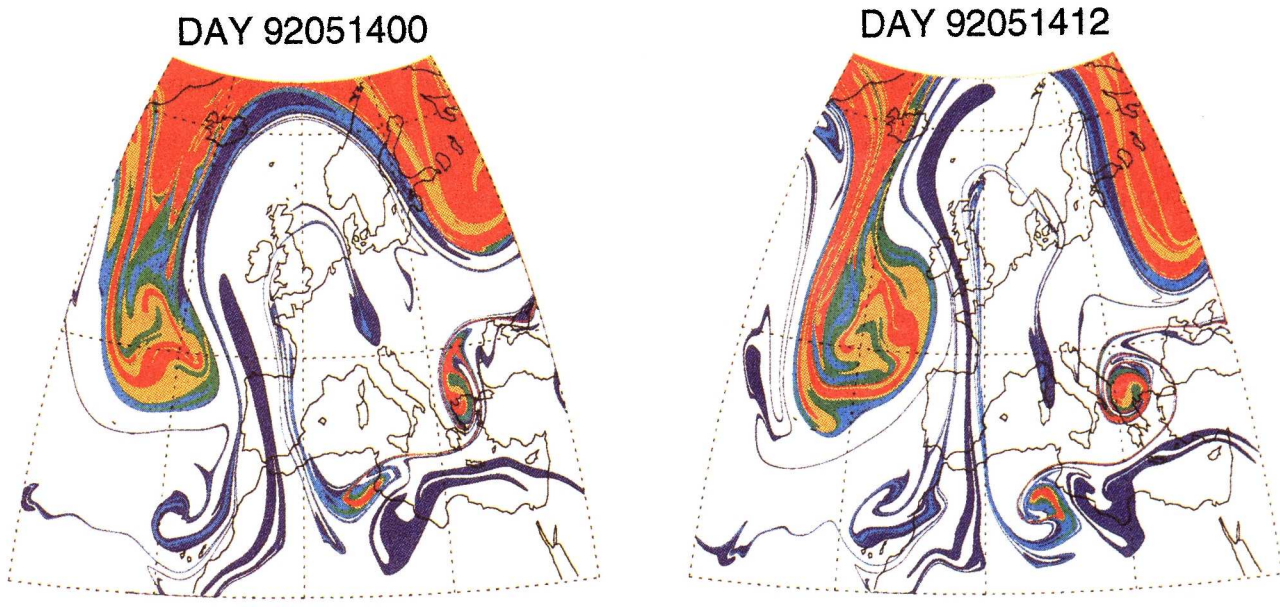
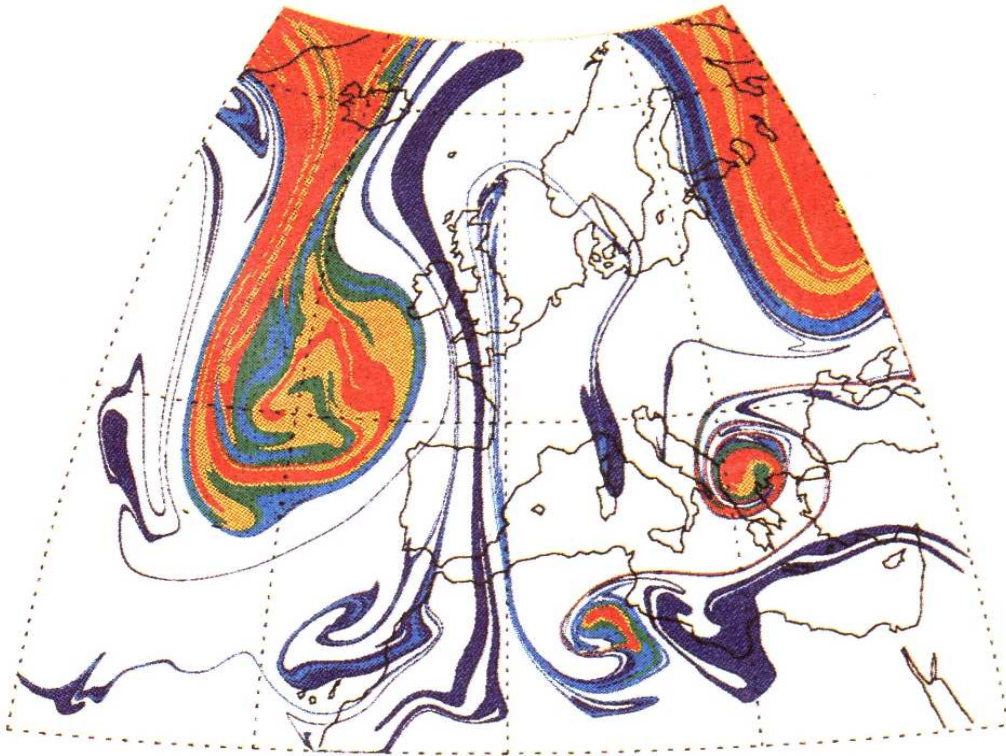
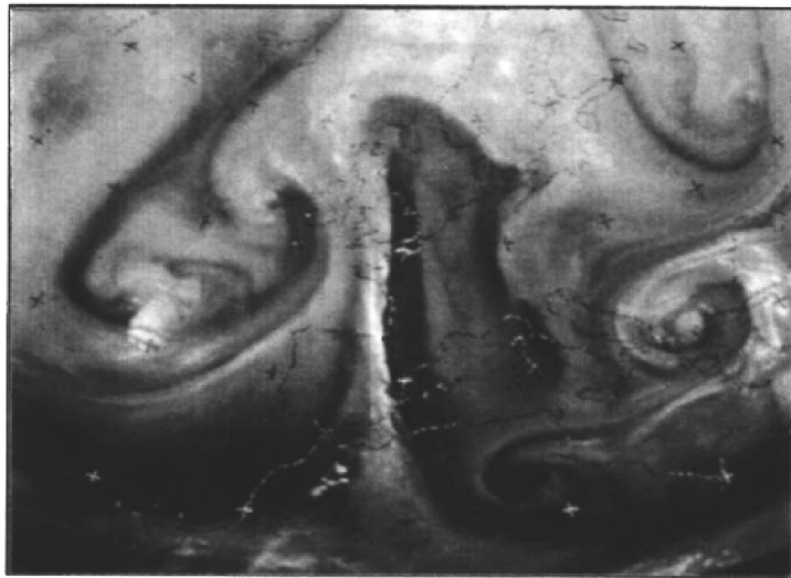


Plate 2. The pattern of select PV contours for the same four times and on the same isentropic surface as the panels in Figure 7, but derived using contour advection.

DAY 92051412



(b)



Meteosat water vapour image 14 May 1992 12:00UT

Figure 1: (a) Passive tracer on 320-K isentropes for May 14 1992, at 1200UT, predicted using a high-resolution Lagrangian tracer-advection algorithm, using winds from meteorological data. The tracer contours were initialized five days earlier to coincide with contours of a dynamical tracer, potential vorticity, that was itself calculated from meteorological data. For more details about potential vorticity, see §2.3. (b) Meteosat 5.7 to 7.1 μm water vapour image. The dark regions signify high radiance values and, in effect, low moisture content in the upper troposphere and lower stratosphere. (Both (a) and (b) taken from Appenzeller et al., 1996.)

Limitations of CAS Diagnostic

- *diagnostic applied as an initial value problem, not a forced/dissipative problem (no sources and sinks)*
- *initialization: structure (filamentation) depends on time that contours are initiated. There is an “art” to the procedure*
- *While the filamentation does not appear to be sensitive to the spatial and temporal resolution of the wind, a careful analysis (Methven and Hoskins 1999) indicates that **displacement errors in filament position** occur which are directly proportional to the spatial and temporal truncation of the winds.*

Methvanen and Hoskins (1999)

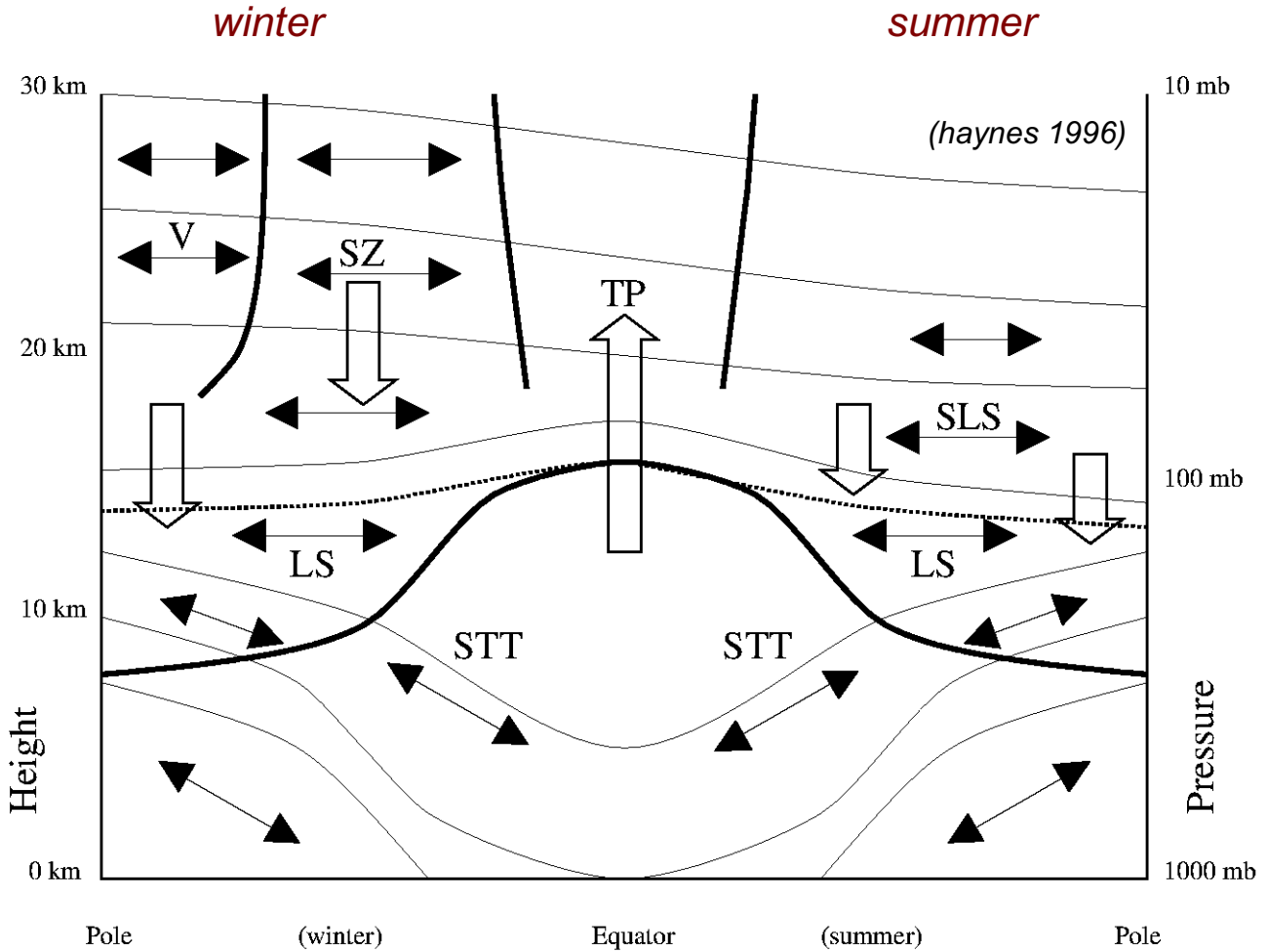
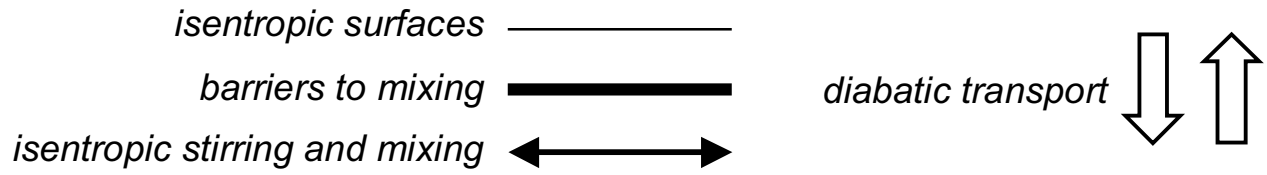
introduce TSF (trustworthy scale factor)

$$TSF = \frac{\text{smallest resolved scale in advecting wind}}{\text{smallest trustworthy scale in tracer field}}$$

$TSF \approx 6.1 \pm 0.3$ *baroclinic wave life cycle*
(based on T341L30 simulations)

$TSF \approx 5.5 \pm 0.5$ *NH winter lower stratosphere*
ECMWF analyses similar procedure
as Waugh and Plumb (1994)

Large-Scale Transport



V – *winter polar vortex*

SZ – *surf zone*

TP – *tropical pipe*

SLS – *summer lower stratosphere*

LS – *lower stratosphere*

STT – *subtropical upper troposphere*

Area Coordinates and Effective diffusivity

(Nakamura 1996)

(Winters and D'Asaro 1996)

Goal: simplify advection diffusion equation:

$$\frac{\partial \chi}{\partial t} + \mathbf{u} \cdot \nabla \chi = \nabla \cdot (\kappa \nabla \chi)$$

so that it is only a diffusion equation

$$\frac{\partial \tilde{\chi}}{\partial t} = \nabla \cdot (\kappa_{eff} \nabla \tilde{\chi})$$

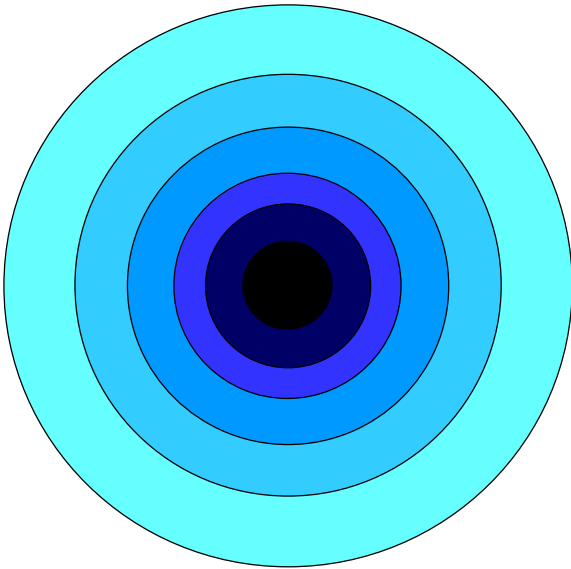
here

$$\chi = \chi(\mathbf{x}, t)$$

$$\tilde{\chi} = \tilde{\chi}(A, t)$$

and

$$A = A(\chi, t) \quad \text{the area enclosed by the contour with concentration: } \chi$$

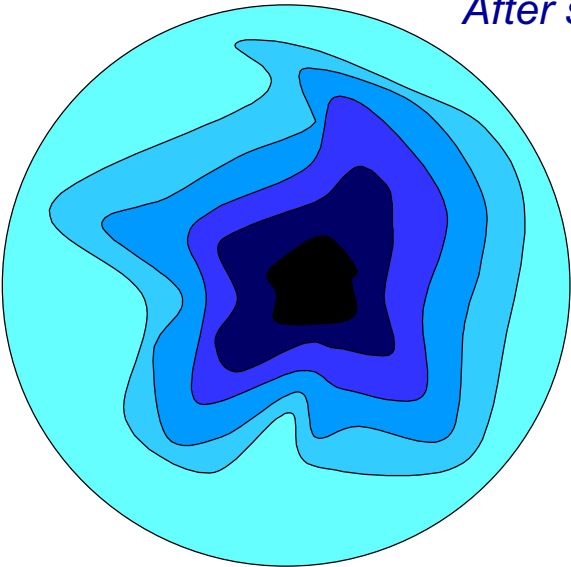


Consider an initial zonally symmetric tracer distribution

each contour encloses a specific area:

$$A_i = \pi R_i^2$$

After some period of Chaotic Advection...

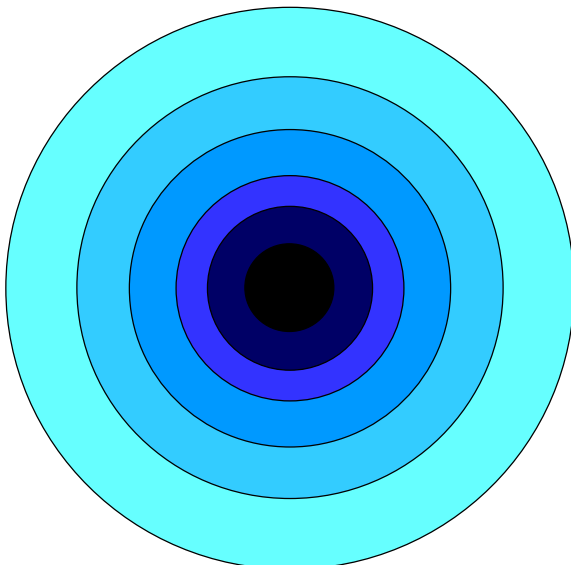


How much irreversible mixing has occurred?

→ determined new area of each contour: \widehat{A}_i

equivalent radius of circular contours:

$$\Rightarrow \widehat{R}_i = \left(\frac{\widehat{A}_i}{\pi} \right)^{1/2}$$



If $\widehat{R}_i = R_i$ or $\widehat{A}_i = A_i$

⇒ no irreversible mixing

(incompressible flow)

Effective Diffusivity and Equivalent Length

advection diffusion equation:

$$\frac{\partial \chi}{\partial t} + \mathbf{u} \cdot \nabla \chi = \nabla \cdot (\kappa \nabla \chi)$$

area coordinates \rightarrow diffusion equation:

$$\frac{\partial \tilde{\chi}(A, t)}{\partial t} = \frac{\partial}{\partial A} \left(\kappa L_e^2 \frac{\partial \tilde{\chi}}{\partial A} \right)$$

where

$$L_e^2(A, t) \equiv \frac{\partial}{\partial A} \iint_{A(\chi, t)} |\nabla \tilde{\chi}|^2 dA \left(\frac{\partial \tilde{\chi}}{\partial A} \right)^{-1}$$

$L_e(A, t)$ – “equivalent length”, the length of the tracer contour of concentration $\tilde{\chi}$

Large values of $L_e(A, t) \Rightarrow$ strongly stirred contours (filaments)

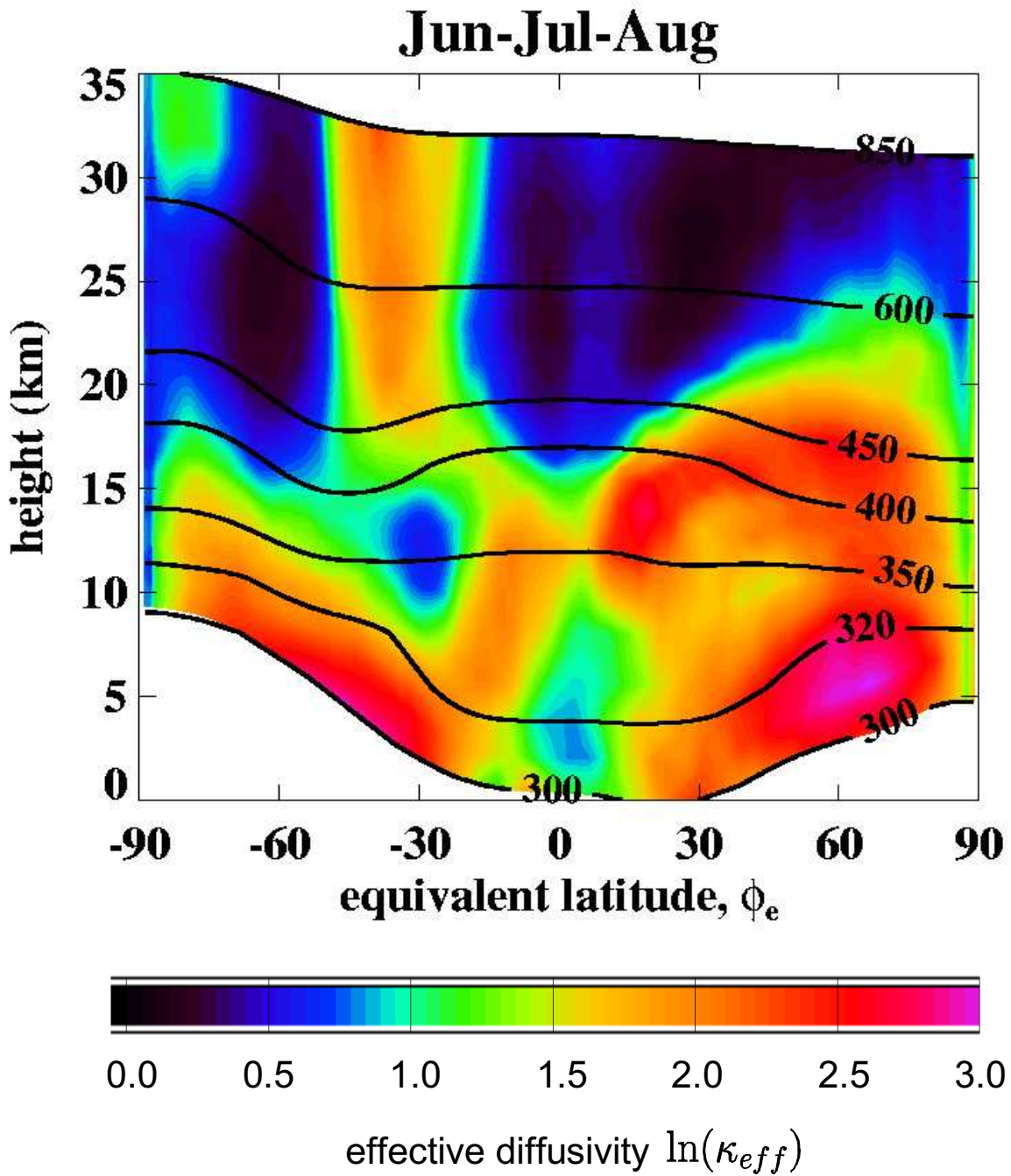
$\kappa_{eff} \equiv \kappa L_e^2(A, t)$ – “effective diffusivity”

Large $\kappa_{eff} \Rightarrow$ strong isentropic mixing

Small $\kappa_{eff} \Rightarrow$ weak isentropic mixing (barriers)

(Haynes and Shuckburgh 2000)

Integration of advection/diffusion equation using ECMWF winds (T42) using a single-layer T82 spectral model.



Utility of Effective Diffusivity

- *improved definition of the tropopause*

minimum value of κ_{eff} in each hemisphere on each isentropic surface between say (300K — 450K)

- *powerful diagnostic to identify and quantitatively compare transport barriers and mixing regions*

useful diagnostic for model validation of transport

- *future goal is to relate values of κ_{eff} to actual fluxes of tracers*

allow possibility to use κ_{eff} to quantify transport